

The magnetism of wurtzite CoO nanoclusters

Ruairi Hanafin, Thomas Archer and Stefano Sanvito
School of Physics and CRANN, Trinity College, Dublin 2, Ireland
(Dated: May 7, 2022)

The possibility that the apparent room temperature ferromagnetism, often measured in Co-doped ZnO, is due to uncompensated spins at the surface of wurtzite CoO nanoclusters is investigated by means of a combination of density functional theory and Monte Carlo simulations. We find that the critical temperature extracted from the specific heat systematically drops as the cluster size is reduced, regardless of the particular cluster shape. Furthermore the presence of defects, in the form of missing magnetic sites, further reduces T_C . This suggests that even a spinodal decomposed phase is unlikely to sustain room temperature ferromagnetism in ZnO:Co.

In recent years the search for ferromagnetism in insulating oxides doped with small quantities of transition metals has become a topic generating much debate in the literature. Taking ZnO:Co as the proto-typical example for this class of materials, many experimental groups have reported room temperature ferromagnetism^{1,2,3}, whereas several other have failed to find any such evidence^{4,5}. Notably, growth conditions, sample morphology and spatial Co distribution play a crucial rôle in determining the magnetic properties. In particular, there is now an emerging view that samples with high structural quality and uniform Co distribution do not result in long-range ferromagnetism at high temperature, and that the magnetism may be related to structural⁶ or point defects⁷.

Given the unsettled experimental landscape it should not surprise that a number of interesting and competing theoretical models have been proposed. In general explanations involving standard mechanisms for the magnetic interaction appear problematic. Schemes leading to short range magnetic coupling such as super-exchange need a Co concentration, $[Co]$, exceeding the percolation threshold. This is around 20 % for an interaction extending to the nearest neighbour sites of an *fcc* lattice, and it is about a factor of 5 larger than the typical experimental concentrations. Similarly carrier mediated mechanisms are not sustained by experimental evidence, which shows both paramagnetism in presence of abundant free carriers⁶ and ferromagnetism deep in the insulating region of the phase diagram². More generally carrier concentration and mobility have an apparent little correlation to the magnetic properties⁸. Furthermore carrier mediated mechanisms are difficult to validate on a solid theoretical ground by using first principles calculations, since the empty Co *d* levels are usually erroneously predicted too shallow at the edge of the ZnO conduction band⁹.

Thus one has to look for more complex mechanisms for the magnetic interaction. Amongst these, the donor impurity band exchange model (DIBE)¹⁰ has enjoyed considerable popularity in the experimental community. According to the DIBE the magnetic interaction among Co^{2+} ions is mediated by donors, whose charge density is localized over large hydrogenic orbitals, so that the relevant percolation threshold becomes that of the

donors and not that of the Co. Unfortunately the model still fails at the quantitative ground, since room temperature ferromagnetism needs prohibitively large exchange coupling between the donors and the $Co^{10,11}$. A second, recently proposed scheme, is the two-species model^{7,12} in which Co-oxygen vacancy pairs (CoV) act as a second magnetic center in addition to Co^{2+} . Interestingly CoV can interact magnetically strongly up to the third nearest neighbours, where the percolation threshold drops to 7 %. Although this is still too high to justify a long-range ferromagnetic order, it suggests that room temperature ferromagnetism can be achieved in samples where Co ions are non-uniformly distributed.

The extreme limit of Co segregation is represented by the formation of some secondary Co-based phase. Usually metallic Co is excluded by X-ray data¹³. Unfortunately all other compounds in the Zn-Co-O phase diagram (CoO , Co_2O_3 , Co_3O_4 , $ZnCo_2O_4$) are either non-magnetic or antiferromagnetic with low Néel temperatures, so that there is no obvious candidate material to form ferromagnetic clusters in ZnO. Still, recently Dietl et al. suggested that the apparent room temperature ferromagnetism in ZnO:Co may be due to uncompensated spins at the surface of CoO nanoclusters maintaining the ZnO wurtzite (WZ) lattice structure¹⁴. Indeed both WZ and zincblende (ZB) CoO were synthesized in the bulk^{15,16,17}, but little magnetic characterization exists. Unfortunately calculations based on density functional theory (DFT) and Monte Carlo (MC) methods are discouraging¹⁸. In fact all the possible CoO polymorphs, including WZ and ZB, do not display a ferromagnetic order but instead they are characterized by a general spin frustration. As a result, the critical temperatures, T_C , extracted from the specific heat are well below room temperature. Notably such a frustration was recently confirmed experimentally¹⁹ for the WZ phase.

However, even if one can exclude magnetism in the bulk, the question of whether or not uncompensated spins can order at the surface of a nanocluster remains open. In particular this is an intriguing question since the dominant exchange parameter extracted from DFT for wurtzite CoO, the one giving frustration, is large. One can then speculate that reducing frustration (as it happens on a surface) can help in enhancing T_C .

Such an open question is investigated here, where we use MC simulations for extracting the thermodynamical properties of WZ CoO nanoparticles of different shapes and dimensions.

I. FOUNDATION OF THE MODEL AND COMPUTATIONAL DETAILS

We perform MC calculations for a classical Heisenberg Hamiltonian of the form

$$H = -\frac{1}{2} \sum_{i,j} J_{ij} \vec{S}_i \cdot \vec{S}_j + \sum_i D \left(\vec{S}_i \cdot \hat{n} \right)^2, \quad (1)$$

where \vec{S}_i is a classical spin located at site i ($|\vec{S}_i| = 3/2$ for Co^{2+}) and J_{ij} is the exchange parameter between spins at sites i and j . The second term in (1) describes the hard-axis easy-plane crystal anisotropy, \hat{n} is a unit vector along the WZ c -axis and the zero-field splitting for Co^{2+} taken from electron paramagnetic resonance²⁰ is $D = 2.76 \text{ cm}^{-1}$.

The values for the various exchange parameters, J , for bulk WZ CoO have been calculated previously¹⁸ from DFT using the LDA+ U extension of the local density approximation (LDA). The procedure used was to fit the total energies of a number of reference DFT calculations for different magnetic supercells to the Hamiltonian of equation (1). For WZ CoO four different J 's are enough to describe the dominant magnetic interaction, with an error over the reference DFT calculations smaller than 1 meV/Co. We have then found: $J_1 = 6.1 \text{ meV}$, $J_2 = -36.7 \text{ meV}$, $J_3 = -0.2 \text{ meV}$, $J_4 = -5.2 \text{ meV}$, where the index n in J_n refers to the neighbour degree (i.e. "1" is for first near neighbours Co^{2+}). The dominant interaction, J_2 , is thus for first nearest neighbours in the $\{001\}$ plane (second nearest neighbours overall) and it is antiferromagnetic. This is the origin of the frustration and of T_C 's below room temperature for the bulk. The same parameters are used for the calculations of finite particles presented here.

The ground state of a given particle is found by the simulated annealing method, since frustration introduces many low energy configurations differing considerably from the ground state but with minor energy differences from it. Such an energy landscape clearly makes the conjugate gradient and the steepest descent schemes ineffective. The temperature dependence is then investigated with Monte Carlo simulations. We use the standard Metropolis algorithm where the acceptance probability of a new state is 100 %, if the new state has an energy lower than that of the old one, and it is given by the Boltzmann factor otherwise. For each different magnetic cluster we equilibrate the system at a given temperature and then extract thermodynamical quantities by sampling over several millions MC steps. In particular we extract T_C from the peak in the specific heat, C . This becomes necessary since an obvious order

parameter is difficult to find for these highly frustrated clusters.

Such a computational scheme is not free of uncertainty. Firstly, the reference DFT calculations are dependent on the specific choice of exchange and correlation function used. LDA+ U is certainly suitable for CoO and our parameterization of the $U - J$ parameter is based on total energy considerations, i.e. on fitting the structural properties and not the band-structure¹⁸. Secondly the Heisenberg model used contains only J 's extending over a limited range and includes only pairwise interaction. The first approximation appears acceptable given the good quality of the fit to DFT, while the second one is more difficult to assess. Nevertheless we have used rocksalt CoO to estimate the error and find that typically our T_C 's for the bulk are underestimated by about 30 %¹⁸. Considering that the Co valence in rocksalt and WZ CoO is the same, we speculate that the same error found for the rocksalt phase can be transferred to WZ.

Still the uncertainty of using bulk parameters for finite clusters simulations remains. However, it is important to bare in mind that here we do not consider free-standing CoO nanoparticles, but instead CoO clusters embedded into a ZnO matrix. This means that the local chemical coordination of each Co atom (i.e. the fourfold coordination to O) in the cluster is identical to that of bulk CoO. Thus the finite size affects only the magnetic coordination and one can safely use bulk parameters for clusters. This, of course, would be inadequate in the case of free surfaces or grain boundaries for which a new parameterization is needed.

II. RESULTS

If present, it is likely that CoO nanoclusters form in ZnO either during the growth process or during post-growth treatment. DFT calculations in fact confirm that there is an energy gain when moving Co ions to nearest neighbouring positions⁷, so that clustering is highly probable. This can possibly be tuned by growth parameters and eventually the presence of additional dopants²¹. Still, even assuming that ZnO:Co during the growth has enough kinetic energy to form large CoO clusters, it is hard to predict whether such clusters should have a preferential shape. Indeed simulations of spinodal decomposition²² seem to suggest the formation of highly Co-rich regions without any particular geometrical structure. This is then a different situation from that of free-standing nanoparticles, where the presence of free surfaces drives the particle geometry. For this reason we have looked at three different particle shapes, namely spherical, cylindrical and perforated spherical. The last ones are spherical particles where a fraction of the Co sites is randomly removed.

1. Spherical Nanoparticles

We consider spherical particles first. These are constructed by simply removing all the atoms beyond a sphere of a give radius, R . In doing so the position of the center of the sphere influences the atomic details of the external surface so that different particles with the same radius can be made. We find that all the particle properties are relatively sensitive to the position of the particle center (chosen within the WZ unit cell) for small particles, but they become progressively center-independent as the radius gets larger. This is expected since larger surfaces allow all the thermodynamical quantities to self-average. For this reason we perform averages over the position of the center only for the smaller particles investigated.

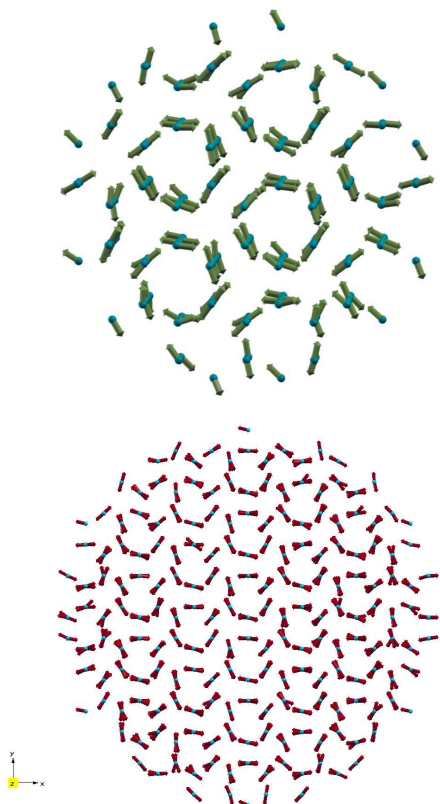


FIG. 1: [Color on line] Ground state spin configuration of spherical particles of different size: 12 Å (top) and 18 Å (bottom). Note the large degree of compensation in the inner core of the particles and the presence of non-compensated spins at their surfaces.

We start our analysis by presenting the ground state spin configuration as calculated with simulated annealing. This is shown in figure 1 respectively for a small ($R = 12$ Å) and a large ($R = 18$ Å) particle. In the figure the particles are oriented with the WZ c -axis pointing perpendicularly to the page, so that the a - b planes are visualized. The figure displays a clear

R (Å)	V (Å ³)	S (Å ²)	N_{Co}	μ/Co (μ_{B})	T_{C}
6	940	452	52	< 0.225	81
7	1436	615	64	< 0.225	100
8	2143	803	94	< 0.18	107
10	4186	1256	174	< 0.18	126
12	7234	1808	324	< 0.09	136
17	20569	3629	920	< 0.045	163
19	28716	4534	1300	< 0.03	169
22	44580	6079	2016	< 0.015	176
29	102109	10562	4634	< 0.0015	187

TABLE I: Table listing the uncompensated magnetic moment per Co in the ground state, μ , and the critical temperature, T_{C} , extracted from the specific heat, for spherical particles of different radius. We also report the number of Co atoms contained in the particle, N_{Co} , and both particle volume, V , and area of the surface, S .

spin compensation of the particle inner core. As for the case of bulk WZ CoO, the strong first nearest neighbour antiferromagnetic constant in the a - b plane, J_2 , drives the frustration. As a result the spins in the a - b plane align at 120° with respect to each other and the net moment per plane vanishes. At the surface the frustration is lifted by translation symmetry breaking and a net uncompensated moment, μ , emerges. Its direction and intensity depends on the particle size, and for small particles on the details of the surface geometry. In any case the moment is always rather small and it is then difficult to visualize by simply looking at figure 1.

In table I we list such a ground state uncompensated magnetic moment (per Co atom) for spherical particles of different sizes. In the table for each radius we report the upper value obtained over a number of different geometrical realizations of the particle. In general the uncompensated magnetic moments are rather small, so that the cluster model itself is at best capable of explaining only weak magnetism in ZnO:Co. The table also allows us to extract an upper limit for the magnetic moment at room temperature due to WZ CoO particles. In fact, by assuming that magnetization reversal is driven by coherent rotation we estimate that particles with radii larger than 15 Å (containing about 800 Co atoms) are large enough to be superparamagnetically blocked at room temperature. Their ground state (at $T = 0$) magnetic moment is calculated between $0.1 \mu_{\text{B}}/\text{Co}$ and $0.05 \mu_{\text{B}}/\text{Co}$ (Table I). Thus, if magnetism originates from CoO clusters with uncompensated spins, then a ferromagnetic signal at room temperature cannot be associated to magnetic moments in excess of $0.1 \mu_{\text{B}}/\text{Co}$. In fact particles with larger μ have a radius smaller than 15 Å, they are not be superparamagnetically blocked at room temperature, and hence they cannot contribute to the ferromagnetic signal. However, even for the possibility of weak ferromagnetism to be sustained one

has to demonstrate that the small magnetic moments survive at room temperature.

Unfortunately for these frustrated system the magnetization is not a good order parameter and no sublattices magnetizations can be identified. Moreover both the uncompensated moment and the particle susceptibility turn out to be rather noisy quantities, so that no T_C can be extracted from them. We then calculate T_C from the analysis of the specific heat, C , as a function of temperature. This is shown in figure 2 for a number of nanoparticles of different radii. The upper curve corresponds to $R = 6 \text{ \AA}$ and the lower to $R = 30 \text{ \AA}$ with the curves in between corresponding to radii incrementing by 1 \AA . From the curves we can clearly

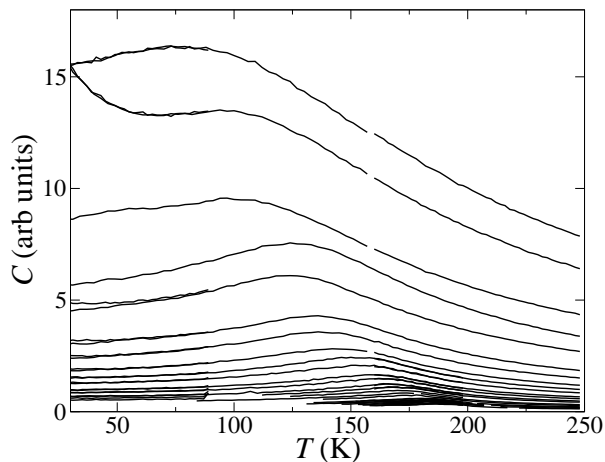


FIG. 2: The specific heat, C , as a function of temperature for finite clusters of wurtzite CoO. The curves are for particles of different radii, ranging from 6 \AA (top) to 30 \AA (bottom), in increment of 1 \AA

identify a peak that becomes more diffuse as the particle size grows. Nevertheless we can still assign to the peak position the T_C of each particle. These are also reported in Tab. I. Interestingly the T_C calculated for bulk WZ CoO with the same parameterization used here is only 160 K^{18} , i.e. it corresponds to a particle with a radius of 16 \AA .

Finite size scaling theory for the Heisenberg model and ferromagnetic interaction^{23,24} predicts a variation of the critical temperature with particle radius of the form

$$\frac{T_\infty - T_C(R)}{T_\infty} = \left(\frac{R}{R_0} \right)^{-\beta}, \quad (2)$$

where R_0 and T_∞ are respectively the correlation radius and the critical temperature for the bulk. This cannot be applied directly to our results since T_∞ is smaller than $T_C(R)$ for large clusters, i.e. the left-hand side of equation (2) becomes negative for some R . We have then fitted the calculated $T_C(R)$ to the equation (2), by assuming a different T_∞ . The results are reported in figure 3. In the curve we show two fits obtained by taking $T_\infty = 200 \text{ K}$ and performing the fit respectively

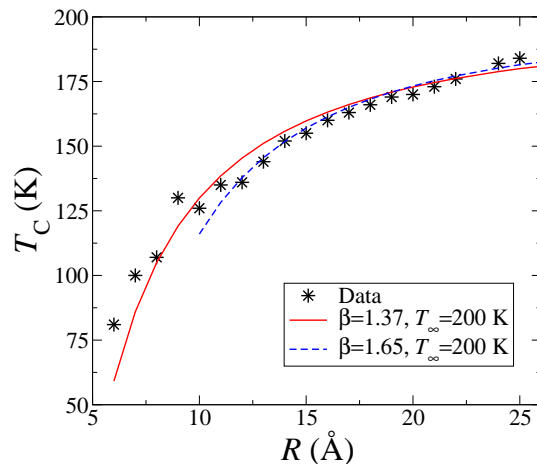


FIG. 3: [Color on line] Critical temperature as a function of the particle radius R (* symbols). The lines are fits to finite size scaling theory [Eq. (2)]. The solid red line corresponds to the fit obtained for $R > 6 \text{ \AA}$, while the dashed blue curve is for $R > 10 \text{ \AA}$.

over the range $R > 6 \text{ \AA}$ (solid red curve) and $R > 10 \text{ \AA}$ (dashed blue curve). As expected the fit improves when particles with small radii are excluded, since the scaling law is strictly valid in the vicinity of T_∞ . In any case we clearly observe that a rather good fit can be obtained for critical exponents in the range of that expected for the Heisenberg model ($\beta \sim 1.42$), when T_∞ is about 200 K . For these values we find a correlation radius of the order of 6 \AA .

We are at this time uncertain of why T_∞ calculated from MC for an infinite system (in practice it is calculated for a finite system with periodic boundary conditions and sufficiently large cells) differs from that extrapolated from finite size scaling. In general $C(T)$ for finite particles is much more diffuse than that calculated by using periodic boundary conditions, so that the assignment of T_C may be affected by some errors. However, such an uncertainty is smaller than the difference between the two temperatures ($\sim 40 \text{ K}$), so that an alternative explanation is needed. We believe that the surface and the core of the particles contribute in a substantial different way to the T_C so that scaling theory cannot be applied directly. In fact, depending on the magnetic coupling at the surface compared to that of the bulk, it was already demonstrated that T_C can either increase or decrease as a function of the particle size^{25,26,27}. This means that depending on the details of the magnetic interaction T_C as a function of the particle size can approach T_∞ asymptotically either from below or from above. In the present case of frustrated interaction it appears that the bulk value is approached in a non-monotonic fashion so that there exists spherical particles with a T_C larger than that of the bulk. This aspect will be further investigated in the next section.

In any case we find that spherical particles, despite

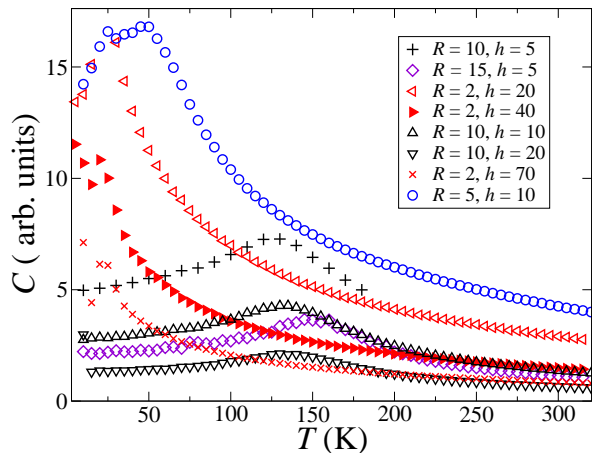


FIG. 4: [Color on line]. Specific heat as a function of temperature for a representative sample of cylindrical nanoparticles with different radii and lengths.

for large radii present a T_C larger than that of the bulk, still fall quite short from being magnetic at room temperature. Furthermore the particles with the largest magnetic moment are those showing the lowest T_C , which makes us concluding that spherical wurtzite Co particles cannot be at the origin of the room temperature magnetism in ZnO:Co.

2. Cylindrical Nanoparticles

In order to further investigate the relative importance of the surface and bulk contributions to the magnetism we consider cylindrical nanoclusters, constructed with the cylinder axis oriented along the WZ c -axis. By varying both the length and radius of such a particle the surface area may be considerably altered whilst the total volume and hence the total number of atoms in the cluster remains constant. In figure 4 we present the specific heat for a number of cylinders of different dimensions, where we can still clearly observe the presence of a peak. As in the case of spherical particles we associated the critical temperature to the peak position.

These are presented next in table II, where we list also the particle volume and the area of the surface. The most relevant feature emerging from the table is the rather sharp dependance of T_C on the particle radius and its insensitivity over its length. This results in the interesting finding that particles presenting the same volume but different aspect ratios can display rather different T_C 's. For example the volume of a particle with $R = 5 \text{ \AA}$ and $h = 30 \text{ \AA}$ is about 30% larger than that of a particle with $R = 10 \text{ \AA}$ and $h = 5 \text{ \AA}$. Nonetheless its T_C is a factor 3 smaller (44 K against 122 K).

In addition we find that the critical temperature of cylindrical nanoparticles becomes almost independent from the length of the cylinder beyond a certain critical

length, h_C . For instance h_C is 2 \AA , 5 \AA , 10 \AA and 20 \AA respectively for R being 2 \AA , 5 \AA , 10 \AA and 15 \AA . Thus it is tempting to propose the empirical relation $h_C \sim R$. As a consequence for particles with $R/h < 1$ there is only one relevant dimension, R . In fact for long cylinders ($R \ll h$) the surface to volume ratio remains constant at $2/R$, so that the magnetic energy density does not change with the cylinder length. This seems to be at the origin of the saturation of T_C with h .

Interestingly for $R = h$ the area of the surface of the cylinder and that of the sphere become identical, while the volumes follow the relation $V_{\text{sphere}} = 4/3 V_{\text{cylinder}}$. In general we expect that the T_C of a nanoparticle has both a surface and a volume contribution. In the case $R = h$ the surface contribution is identical for spheres and cylinders, while the volumetric contribution is expected to be larger for the cylinders, since these have a larger volume. Thus we expect that the T_C of a sphere of radius R is lower than that of a cylinder of radius R and $h = R$, as indeed confirmed by comparing the tables I and II.

Finally we take a look at the magnetization, finding that this is always small, typically $< 10^{-3} \mu_B/\text{Co}$, and varies little with either changes in the particle dimensions or with the temperature. In summary, from our analysis it does not appear that cylindrical nanoparticles, similarly the spherical ones, are supportive of room temperature ferromagnetism.

3. Perforated Spherical Nanoparticles

Since empty Co sites in a CoO nanoparticle may serve to lift the spin frustration by eliminating a fraction of the neighbours of each Co atom, it is worth analyzing the dependence of T_C over the Co concentration. This essentially corresponds to studying a random ZnO:Co alloy with large Co doping. In general we expect that, as long as the Co concentration exceeds the percolation threshold for the wurtzite lattice (19 % for nearest neighbour interaction), a magnetic order will be found. The question remaining is whether or not magnetization and T_C will increase with respect to their values for stoichiometric CoO when the Co concentration is reduced.

The nanoparticles investigated here are constructed by taking one of the previously made spherical nanocrystals and then removing a chosen fraction of magnetic ions at randomly chosen sites. We consider particles with a radius of 19 \AA , which are large enough to show a substantial T_C , but not enough for the thermodynamical properties to saturate at their bulk values, i.e. the surface of the particles still makes a non-negligible contribution. Furthermore we find that particles with smaller radii are too sensitive to Co vacancies, to the extent that in general at Co concentrations below 90% a T_C is not easily located. Note that, although we name Co vacancy a site where the Co ion is removed, the parameterization for the exchange interaction remains the one calculated for

$R h$	2	5	10	20	30	40	60
2	16 _(25,50)	18 _(63,88)	21 _(125,150)	20 _(251,276)	20 _(377,402)	21 _(502,527)	23 _(754,779)
5	26 _(157,219)	46 _(392,314)	46 _(785,471)		44 _(2355,1099)		
10	102 _(628,753)	122 _(1570,942)	135 _(3140,1256)	135 _(6280,1884)	135 _(9420,2512)	138 _(12560,3140)	138 _(18840,4396)
15	122 _(1413,1601)	152 _(3532,1884)	160 _(7065,2355)	167 _(14130,3297)	170 _(21195,4239)	171 _(28260,5181)	
25	128 _(3925,4239)	158 _(9812,4710)	171 _(19625,5495)	181 _(39250,7065)			
30	130 _(5652,6029)	165 _(14130,6594)	183 _(28260,7536)	191 _(56520,9420)			

TABLE II: The calculated T_C for a number cylindrical nanoparticles with different radius, R , and length, h . The radius is along the vertical axis and the length is along the horizontal one (both in Å). In brackets we report respectively the cylinder volume (Å³) and surface area (Å²).

the perfectly crystalline CoO phase¹⁸, so that the atom removal has only geometrical effects.

Our results are presented in Fig. 5 where we show the specific heat as a function of temperature for different Co concentrations, [Co]. In the same figure we also report the extracted T_C 's as a function of [Co]. The most notable feature is that the peak in $C(T)$ shifts towards lower temperatures and gets broader as Co atoms are removed. This means that the presence of defects reduces the critical temperature, so that lifting locally the frustration does not help in improving the magnetic properties. We find that T_C decreases linearly with the fraction of vacant sites and extrapolates to $T_C = 0$ for [Co]=30%, which is larger than the nearest neighbour percolation threshold. This, however, should not be surprising since deviation from the linear dependence are expected at low [Co]. Interestingly such a linear dependance of T_C on the defect concentration has been reported previously in both experimental and theoretical studies for Ni-Cu alloys^{27,28}

Finally we observe that none of the structures investigated present magnetizations greater than $0.003 \mu_B/\text{Co}$ above 100 K. We then conclude that the breaking of frustration by means of defects appears to have little impact on the magnetization and as a consequence perforated nanoclusters do not appear to sustain any room temperature ferromagnetism.

III. CONCLUSIONS

The focus of this paper was to test the feasibility of the proposal that uncompensated spins on the surface of CoO nanoclusters embedded in ZnO are responsible for the measured magnetic properties of ZnO:Co. Previously we have demonstrated that bulk wurtzite CoO displays a high degree of frustration so that no net magnetization is found even at low temperature. Furthermore the T_C calculated from the peak in the specific heat is substantially lower than room temperature.

The present study has revealed that finite sized clusters are no more promising. Although the frustration is lifted at the interface, we found that usually the finite

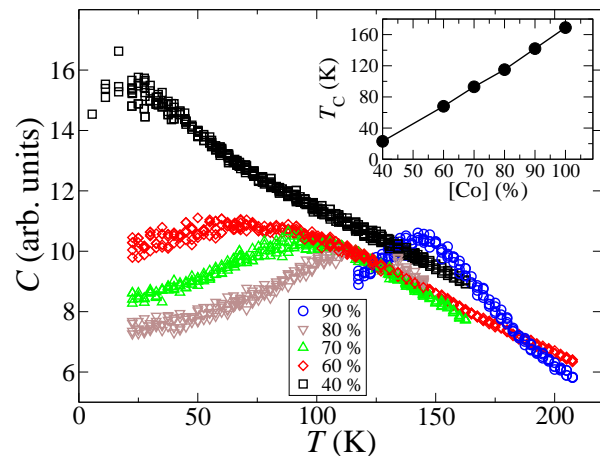


FIG. 5: [Color on line] Specific heat against temperature curves for a perforated nanosphere of radius 19 Å and various Co concentrations, [Co]. We can clearly observe that by reducing the Co content the peak in $C(T)$ moves to lower temperature and gets broader. In the inset we show T_C as a function of [Co] as extracted from the specific heat.

size reduces the critical temperature for magnetism with respect to its bulk value. This happens regardless of the shape of the particle and of the presence of Co empty sites. For some relatively large spherical and cylindrical nanoparticles we have found a marginal enhancement of T_C with respect to bulk, for which we speculate on a non-monotonic dependence of T_C with particle size. In any case the residual magnetizations originating from the finite size remain extremely small at any temperature, so that finite particles can hardly be considered at the origin of the claimed ferromagnetism of ZnO:Co.

In concluding we wish to remark once again that our model is based on a parameterization of the magnetic interaction rooted in DFT calculations for bulk CoO. It is indeed possible that such an interaction is substantially altered at surfaces, so that much larger exchange constants may be found either at grain boundaries or at free surfaces or at the interfaces with the substrate. This can promote residual ferromagnetism. Furthermore

our present model does not include intrinsic defects, which can both alter the local magnetic coupling or form

complexes with Co which may interact over a long range⁷.

-
- ¹ M. Venkatesan, C.B. Fitzgerald, J.G. Lunney and J.M.D. Coey, *Phys. Rev. Lett.* **93**, 177206 (2004).
- ² A.J. Behan, A. Mokhtari, H.J. Blythe, D. Score, X.-H. Xu, J.R. Neal, A.M. Fox and G.A. Gehring, *Phys. Rev. Lett.* **100**, 047206 (2008).
- ³ K.R. Kittilstved, N.S. Norberg and D.R. Gamelin, *Phys. Rev. Lett.* **94**, 147209 (2005).
- ⁴ M. Bouloudenine, N. Viart, S. Colis, J. Kortus and A. Dinia, *Appl. Phys. Lett.* **87**, 052501 (2005).
- ⁵ S. Deka, R. Pasricha and P.A. Joy, *Phys. Rev. B* **74**, 033201 (2006).
- ⁶ T.C. Kaspar, T. Droubay, S.M. Heald, P. Nachimuthu, C.M. Wang, V. Shutthanandan, C.A. Johnson, D.R. Gamelin and S.A. Chambers, *New J. Phys.* **10**, 055010 (2008).
- ⁷ C.D. Pemmaraju, R. Hanafin, T. Archer, H.B. Braun and S. Sanvito, *Phys. Rev. B* **78**, 054428 (2008).
- ⁸ N. Khare, M.J. Kappers, M. Wei, M.G. Blamire and J.L. MacManus-Driscoll, *Adv. Mat.* **18**, 1449-1452 (2006).
- ⁹ S. Sanvito and C.D. Pemmaraju, *Phys. Rev. Lett.* **102**, 159701, (2009).
- ¹⁰ J.M.D. Coey, M. Venkatesan and C.B. Fitzgerald, *Nature Materials* **4**, 172 (2005).
- ¹¹ R. Hanafin and S. Sanvito, *J. Magn. Mater.* **316**, 218 (2007).
- ¹² R. Hanafin, C.D. Pemmaraju and S. Sanvito, *J. Magn. Mater.* (2009), in press.
- ¹³ J.M.D. Coey, *Curr. Opin. Solid State Mater. Sci.* **10**, 83 (2006)
- ¹⁴ T. Dietl, T. Andrearczyk, A. Lipińska, M. Kiecana, M. Tay and Y. Wu, *Phys. Rev. B* **76**, 155312 (2007).
- ¹⁵ M. J. Redman and E. G. Steward. *Nature*, **193** 867, (1962).
- ¹⁶ R. W. Grimes and A. N. Fitch. *J. Mater. Chem.* **1**, 461 (1991).
- ¹⁷ R. W. Grimes and K.P.D. Lagerlof. *J. Am. Ceramic Soc.*, **74**, 276 (1991).
- ¹⁸ T. Archer, R. Hanafin and S. Sanvito, *Phys. Rev. B* **78** 014431 (2008).
- ¹⁹ J. Alaria, N. Cheval, K. Rode, M. Venkatesan and J.M.D. Coey, *J. Phys. D: Appl. Phys.* **41**, 135004 (2008).
- ²⁰ P. Sati, R. Hayn, R. Kuzian, S. Regnier, S. Schafer, A. Stepanov, C. Morhain, C. Deparis, M. Laugt, M. Goiran and Z. Golacki, *Phys. Rev. Lett.* **96**, 017203 (2006).
- ²¹ T. Dietl, *Nature Materials* **5**, 673 (2006).
- ²² K. Sato, T. Fukushima and H. Katayama-Yoshida, *J. Phys.: Condens. Matter* **19**, 365212 (2007).
- ²³ K. Chen, A.M. Ferrenberg and D.P. Landau, *Phys. Rev. B* **48**, 3249 (1993)
- ²⁴ T. Ambrose and C.L. Chien, *Phys. Rev. Lett.* **76**, 1743 (1996).
- ²⁵ A. Ayuela and N.H. March, *Phase Trans.* **81**, 387 (2008).
- ²⁶ D. Weller, S.F. Alvarado, W. Gudat, K. Schröder and M. Campagna, *Phys. Rev. Lett.* **54**, 1555 (1985).
- ²⁷ I. Apostolova and J.M. Wesselinowa, *Solid State Communications* **149**, 986 (2009).
- ²⁸ J. Kudrnovsky, V. Drchal and P. Bruno, *Phys. Rev. B* **77**, 224422 (2008).